Crossover from three-dimensional to two-dimensional systems in the nonequilibrium zero-temperature random-field Ising model

Djordje Spasojević and Svetislav Mijatović
Faculty of Physics, University of Belgrade, POB 368, 11001 Belgrade, Serbia

Víctor Navas-Portella
Centre de Recerca Matematica, Edifici C, Campus Bellaterra, E-08193 Bellaterra, Catalonia, Spain; Barcelona Graduate School of Mathematics (BGSMath), Edifici C, Campus Bellaterra, E-08193 Barcelona, Spain; and Facultat de Matemàtiques i Informàtica, Universitat de Barcelona, Gran Via de les Corts Catalanes, 585, E-08007 Barcelona, Spain

Eduard Vives
Departament de Matèria Condensada, Facultat de Física, Universitat de Barcelona, Diagonal 645, 08028 Barcelona, Catalonia, Spain

(Received 1 August 2017; published 10 January 2018)

We present extensive numerical studies of the crossover from three-dimensional to two-dimensional systems in the nonequilibrium zero-temperature random-field Ising model with metastable dynamics. Bivariate finite-size scaling hypotheses are presented for systems with sizes $L \times L \times l$ which explain the size-driven critical crossover from two dimensions ($l = \text{const}$, $L \to \infty$) to three dimensions ($l \propto L \to \infty$). A model of effective critical disorder $R_c^{\text{eff}}(l, L)$ with a unique fitting parameter and no free parameters in the $R_c^{\text{eff}}(l, L \to \infty)$ limit is proposed, together with expressions for the scaling of avalanche distributions bringing important implications for related experimental data analysis, especially in the case of thin three-dimensional systems.

DOI: 10.1103/PhysRevE.97.012109

I. INTRODUCTION

In the world of emerging novel technologies thin three-dimensional systems (ribbons, thin films, layered materials, etc.) play a prominent role. Having one spatial dimension much smaller than the remaining two, thin three-dimensional systems stand between the true three-dimensional (3D) and two-dimensional (2D) systems. So, the question arises what regularities are shown in their behavior on the 3D to 2D crossover, which is of considerable significance for proper interpretation and understanding of experimental (e.g., Barkhausen noise [1]) data, and their usage in future devices.

Such devices (sensors, actuators, coolers, energy harvesting devices, etc.) have to be designed taking into account the response to external driving of the embedded thin 3D systems (ferromagnets, ferroelectrics, ferroelastics, superconductors, etc). This response depends on the features of phase diagrams (lines of first-order phase transition and critical points) that show a crossover as the aspect ratios of linear dimensions vary.

The dimensional crossover has been studied so far both experimentally [2,3] and in equilibrium models [4–8]; for some other effects of sample geometry on system behavior, see [9,10]. Thus, in equilibrium models it has been established that the systems with constant thickness l, and two diverging spatial dimensions $L \to \infty$, behave in the asymptotic limit essentially as 2D systems, showing a critical temperature $T_c(l)$ that shifts from the critical temperature of the planar 2D system, $T_c(l = 1) = T_c^{2D}$, to the critical temperature of the bulk 3D system, $T_c(l \to \infty) = T_c^{3D}$. For large l, a first approximation for this crossover function should be $T_c(l) - T_c^{3D} \sim l^{1/\nu_{3D}}$, where ν_{3D} is the critical exponent that controls the divergence of the correlation length in three dimensions. Better approximations, improving the ł range of validity of such an expression, have been discussed by several authors [2,8].

On the other hand, much less effort has been made in the understanding of the 3D-2D crossover in out-of-equilibrium systems. Many such systems with ferroic interactions behave athermally, i.e., when driven, they evolve following metastable branches with hysteresis. In many cases, thermal fluctuations might be irrelevant, preventing such systems from reaching equilibrium and leading, in the final consequence, to the critical behavior that is not in the same universality class with that of the equilibrium athermal random-field Ising model (RFIM) systems [11].

In this paper we extend the analysis of the size-driven 3D-2D crossover to metastable out-of-equilibrium critical systems. For this purpose, we will focus our paper on the $T = 0$ RFIM with metastable dynamics (see [12,13] and the references therein), that displays disorder induced criticality both in three dimensions [14] and two dimensions [15].

The paper is organized as follows. The considered variant of the RFIM model is briefly described in Sec. II. In Sec. III, the scaling of avalanche distributions for equilateral lattices is given in Sec. III A, and the scaling of avalanche distributions for nonequilateral lattices is proposed in Sec. III B. Variation of the critical disorder with system thickness is analyzed in Sec. III C, and the collapsing of size distributions in Sec. III D. The main text ends with a discussion of possible consequences on interpretation of experimental data in Sec. IV, and a conclusion in Sec. V. Finally, in Appendix A we give a description of

the details of determination of the number of 2D spanning avalanches and effective critical disorder, while the collapsing of the integrated size distributions in the whole $l/L = \text{const}$ range is illustrated in Appendix B, and the scaling of the distributions of avalanche durations and avalanche energies is proposed in Appendix C.

II. MODEL

The RFIM describes ferromagnetically coupled classical spins $S_i = \pm 1$, located at the sites i of some underlying lattice. The spins are subjected to a homogeneous external magnetic field H, and to a quenched local magnetic field h_i, varying randomly from site to site. Its values h_i are chosen from some distribution, in our case the Gaussian distribution $\rho(h) = \frac{1}{\sqrt{2\pi}R} \exp(-\frac{h^2}{2R^2})$, so that at each site i the expected value of the random field is $\langle h_i \rangle = 0$, while the correlation between the values of the random field taken at any two sites i and j is $\langle h_i h_j \rangle = R^2 \delta_{i,j}$; the width $R = \langle h_i^2 \rangle^{1/2}$ of the distribution of the random field characterizes the amount of disorder in the system, and from now on will be simply referred to as disorder.

The RFIM Hamiltonian in the simplest case reads

$$\mathcal{H} = -\sum_{\langle i,j \rangle} S_i S_j - H \sum_i S_i - \sum_i h_i S_i, \qquad (1)$$

where $\sum_{\langle i,j \rangle}$ denotes summation over all pairs of nearest neighbors $\langle i,j \rangle$. Thus, each S_i is subjected to the effective magnetic field $h_i^{\text{eff}} = \sum_j S_j + H + h_i$, which includes the contribution $\sum_j S_j$ from the nearest neighbors of S_i.

In the nonequilibrium model at $T = 0$, all spins follow the local dynamical rule: when externally driven by H, each spin S_i aligns with the sign of h_i^{eff}. This gives rise to a hysteretic, out-of-equilibrium, avalanchelike response of the system. In the adiabatic regime, H is infinitely slowly varied (here increased) until only the least stable spin is triggered, and subsequently kept constant during the emerging avalanche. Regarding initial and final conditions, each simulation (like ours) may start from $H = -\infty$, when all $S_i = -1$, and stop when all $S_i = +1$. The simulations are repeated many times with different configurations of local magnetic field h_i taken from the same distribution.

III. SCALING OF AVALANCHE DISTRIBUTIONS

A. Equilateral lattices

During the past 25 years, extensive simulations of the $T = 0$ nonequilibrium RFIM have been performed on d-dimensional cubic lattices L^d which are equilateral (i.e., have the same size L along each of the lattice spatial dimensions). These simulations have shown that the model exhibits the mean-field criticality for $d \geqslant 6$ [13,16], and a critical non-mean-field behavior for $2 \leqslant d \leqslant 5$, described by a set of critical exponents and critical parameters that depend on system dimensionality [13–15,17].

The criticality of the RFIM on L^d lattices is controlled in the adiabatic regime by the distance to the critical disorder $R_c^{(d)}$, separating the ferromagnetic $R < R_c^{(d)}$ from paramagnetic $R > R_c^{(d)}$ phase in the $L \to \infty$ limit. For finite L, the distributions of various avalanche parameters follow finite size scaling (FSS) and power laws. In the case of avalanche size S (i.e., number of spins flipped during the avalanche), its distribution $D^{(\text{int})}(S; r, 1/L)$ integrated along the external field H fulfills

$$D^{(\text{int})}(S; r, 1/L) = S^{-(\tau+\sigma\beta\delta)} \bar{\mathcal{D}}_{\pm}^{(\text{int})}(S^{\sigma}|r|, S^{\sigma\nu}/L)\,. \qquad (2)$$

Here, τ, σ, β, δ, and ν are the critical exponents, the reduced disorder $r = 1 - R_c^{(d)}/R$ measures the distance to $R_c^{(d)}$, while $\bar{\mathcal{D}}_{+}^{(\text{int})}$ is the universal scaling function for the size distribution $D^{(\text{int})}(S; r, 1/L)$ for $r > 0$, and $\bar{\mathcal{D}}_{-}^{(\text{int})}$ is the universal scaling function for the size distribution $D^{(\text{int})}(S; r, 1/L)$ for $r < 0$, see [13,14]; like $R_c^{(d)}$, the values of all exponents and the shape of $\bar{\mathcal{D}}_{\pm}^{(\text{int})}$ that appear in (2) depend on system dimension d, but this is omitted for simpler notation. Note that the scaling variable r is normalized by R and not by $R_c^{(d)}$. This nonstandard choice is known to be very adequate for such zero-temperature disorder induced critical points [13,18]. First order expansions in r allow an accurate description of the system properties very far from R_c. This feature, which is not fully understood, is clearly different from what happens in thermal critical points.

B. Nonequilateral lattices

If the system is not equilateral, but has different sizes $L_1, L_2, \ldots, L_d$ along its spatial dimensions, then the FSS of size distribution (2) should instead be given by the expression

$$D^{(\text{int})}(S; r, 1/L_1, 1/L_2, \ldots, 1/L_d) = S^{-(\tau+\sigma\beta\delta)} \times \bar{\mathcal{D}}_{\pm}^{(\text{int})}(S^{\sigma}|r|, S^{\sigma\nu}/L_1, S^{\sigma\nu}/L_2, \ldots, S^{\sigma\nu}/L_d)\,, \qquad (3)$$

having the same scaling along all spatial dimensions due to model isotropy.

In our study of 3D to 2D crossover we have performed extensive simulations on cubic $L \times L \times l$ lattices, having equal length L (in what follows, simply *span*) along two spatial dimensions (say, x and y), and a different thickness l along the third, i.e., z dimension. Values of L range from 256 to 16 384, and values of l range from 2 to 1024 [19]. We used periodic boundary conditions along x and y, and open boundary conditions along the z dimension. Thus, spins in the upper and lower layers have only five neighbors.

In Fig. 1(a), we show the integrated size distributions for 3D systems with same span $L = 8192$, same disorder $R = 2.3$, but various thickness l. As R exceeds the critical disorder $R_c^{3D} = 2.16$ for equilateral 3D cubic lattices [14], the distributions show a clear exponential damping, corresponding to the paramagnetic regime with only small avalanches.

The shape of distributions becomes, however, qualitatively different for disorders below R_c^{3D} and small thicknesses l [see Fig. 1(b)]. In this case many avalanches reach the linear size $l_a > l$ and, being squeezed between the top and the bottom system's surface, effectively behave as if they are 2D avalanches spreading over a 2D lattice. On the other hand, avalanches of small linear size ($<l$) are not affected by the lattice thickness and behave like ordinary 3D avalanches.

Therefore, one can see two portions in the shape of distributions: The left part resembling the distribution of small 3D avalanches and the right tail which, containing quasi-2D

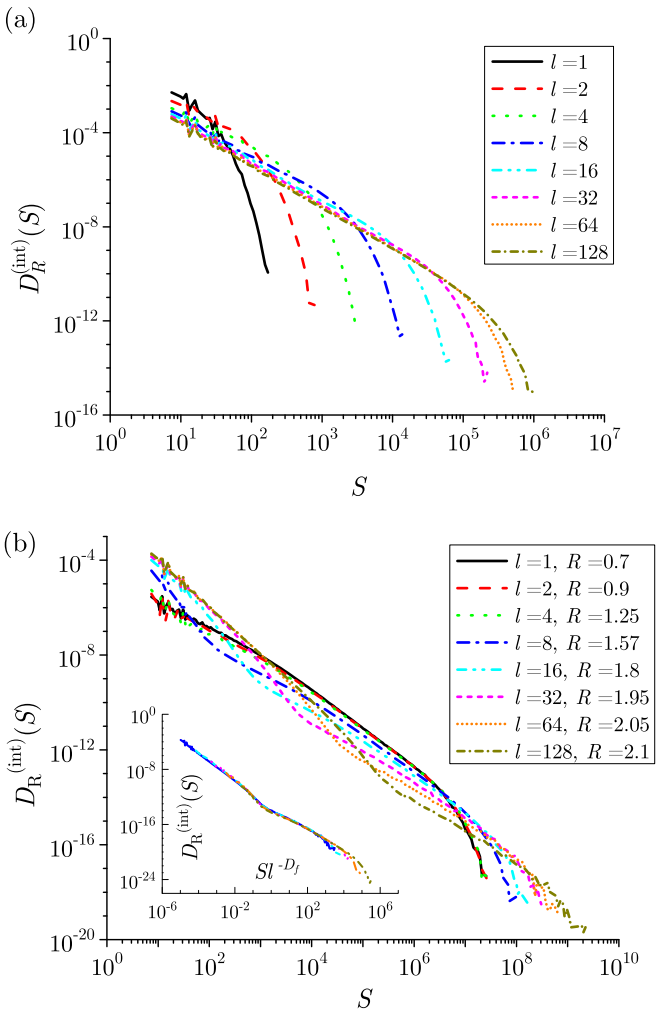

FIG. 1. (a) Integrated size distributions $D_R^{(\mathrm{int})}(S)$ vs avalanche size S obtained for the same disorder $R = 2.3$ and same span $L = 8192$, but various thickness l, shown in the legend. (b) The same as in (a), but for disorders slightly above the effective critical disorder $R_c^{\mathrm{eff}}(l,L)$ for $L \times L \times l$ systems. Inset: When shown vs S/l^{D_f}, the foregoing distributions partially collapse showing branching tails because the values of R and L are not adjusted as is required by (5).

avalanches, becomes more and more similar to the 2D distributions as the system becomes thinner and thinner.

The linear size of the largest small avalanche in thin 3D systems is proportional to the system thickness l. So, the maximum size S of such avalanches, see inset in Fig. 1(b), should be

$$S_{\max} \propto l^{D_f} , \tag{4}$$

where $D_f = 1/\sigma\nu = 2.78$ is the fractal dimension of non-spanning avalanches in three dimensions [18], suggesting the scaling

$$D^{(\mathrm{int})}(S; r, 1/L, 1/L, 1/l) = l^{-(\tau+\sigma\beta\delta)D_f} D^{(\mathrm{int})}(S/l^{D_f}; rl^{1/\nu}, l/L, l/L, 1) \tag{5}$$

of the integrated size distribution with all critical exponents (namely, τ, σ, β, δ, and ν) for the 3D model [13,14].

This equation indicates that, in order to obtain a proper collapsing of the integrated size distributions for different thicknesses l, one should adjust the values of reduced disorders r and spans L so as to keep the terms $rl^{1/\nu}$ and l/L constant. The adjustment of r is not as simple, because here one encounters the question of what should be the critical disorder. In fact, in 3D to 2D crossover, we are dealing with a family of systems specified by their thickness l. Our data corroborate that each such family has its own critical disorder $R_c(l)$, necessary to find the reduced disorder r.

C. Critical disorder

The critical disorder $R_c(l)$ characterizes $L \times L \times l$ systems when they become infinite in the $L \to \infty$ limit. In the ferromagnetic phase of such infinite systems infinite avalanches appear, causing a jump in magnetization ΔM_R that vanishes when $R \to R_c(l)$. For finite L, the role of infinite avalanches is played by spanning avalanches, which are in the case of L^d lattices defined as the avalanches that span the system along at least one of its dimensions (see [12–14,18,20]). This definition ceases, however, to be appropriate for thin $L \times L \times l$ systems where avalanches are more likely to span the system along the (small) z dimension, and improbably along the remaining two (large) dimensions. Therefore, we will consider an avalanche as 2D spanning in the $L \times L \times l$ case if it spans the system along *one or both* of the first two (large) dimensions x and y.

Now, let $N(R; l, L)$ be the *average* number (per run) of 2D spanning avalanches on $L \times L \times l$ systems with disorder R. For fixed l and L, this number, taken as a function of disorder R, has a transition region in which $N(R; l, L)$ can be described by the two-parameter model function

$$N_{R_0,W}(R) = 0.5 \times \mathrm{erfc}[(R - R_0)/W] , \tag{6}$$

with the position of the inflection point R_0 being an estimation of the effective critical disorder $R_c^{\mathrm{eff}}(l,L)$ for finite systems (see details in Appendix A). In Fig. 2 the dots show the so obtained values of $R_c^{\mathrm{eff}}(l,L)$ versus thickness l and span L of the $L \times L \times l$ lattice.

Besides $R_c^{\mathrm{eff}}(l,L)$, Fig. 2 also shows the surface that is our theoretical FSS prediction of how the effective critical disorder should depend on thickness l and span L:

$$R_c^{\mathrm{th}}(l,L) = R_c^{\mathrm{3D}}\left[1 - \frac{\Delta}{l^{1/\nu_{\mathrm{3D}}}} - \frac{(A-\Delta)l^{1/\nu_{\mathrm{2D}}}}{L^{1/\nu_{\mathrm{2D}}} l^{1/\nu_{\mathrm{3D}}}}\right]^{-1} . \tag{7}$$

Here, $1/\nu_{\mathrm{3D}} = 0.71$ [14] and $1/\nu_{\mathrm{2D}} = 0.19$ [15] are the exponents controlling the divergence of the correlation lengths in three and two dimensions, $\Delta \equiv 1 - R_c^{\mathrm{3D}}/R_c^{\mathrm{2D}} \cong -3.0$ measures the relative distance between the critical disorders $R_c^{\mathrm{3D}} = 2.16$ [14] and $R_c^{\mathrm{2D}} = 0.54$ [15] for equilateral 3D and 2D cubic lattices, respectively, while A is the only adjustable parameter.

The physical reasoning behind Eq. (7) is based on the following two arguments.

(i) First, when considering the systems with a fixed aspect ratio $a = l/L$, one gets

$$1 - \frac{R_c^{\mathrm{3D}}}{R_c^{\mathrm{eff}}(aL,L)} = \frac{a^{-1/\nu_{\mathrm{3D}}}}{L^{1/\nu_{\mathrm{3D}}}}[\Delta + (A-\Delta)a^{1/\nu_{\mathrm{2D}}}]. \tag{8}$$

This corresponds to the expected FSS expansion for 3D systems when $L \to \infty$ with an amplitude that depends only

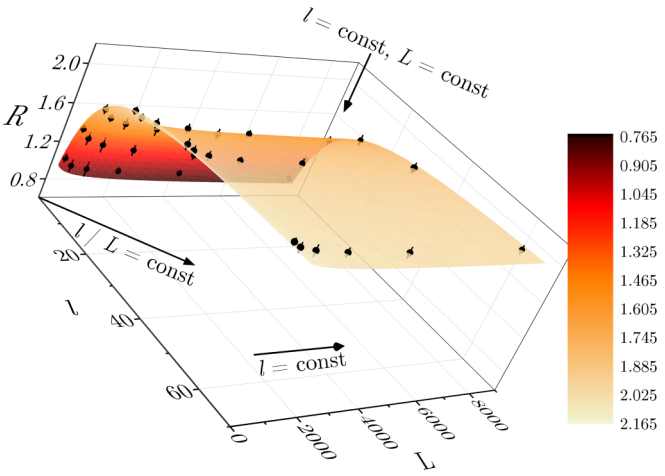

FIG. 2. Numerical estimations of the effective critical disorder $R_c^{\rm eff}(l,L)$ vs thickness l and span L (black balls; error bars are magnified by a factor of 5 for better visibility). The surface shows our theoretical prediction (7). Arrows show three types of characteristic directions that are used for the FSS analysis: $l/L = \text{const}$, $l = \text{const}$ (variable L), and both l, L constant (but variable R).

on the aspect ratio a. Note that for $a = 1$ the term in the square brackets becomes A, and that similar dependence has been found in a recent study of the influence of aspect ratio on the 2D RFIM [9].

(ii) Second, for a system with a fixed thickness l, and after some algebra, one can rewrite expression (7) as

$$1 - \frac{R_c^{\rm 3D}/\left(1-\frac{\Delta}{l^{1/\nu_{\rm 3D}}}\right)}{R_c^{\rm eff}(l,L)} = \frac{1}{L^{1/\nu_{\rm 2D}}}\left[\frac{(A-\Delta)l^{1/\nu_{\rm 2D}}}{l^{1/\nu_{\rm 3D}}-\Delta}\right] \qquad (9)$$

and identify the numerator of the second term on the left-hand side as $R_c(l)$:

$$R_c(l) = \frac{R_c^{\rm 3D}}{1-\frac{\Delta}{l^{1/\nu_{\rm 3D}}}} \Longrightarrow \frac{R_c(l)-R_c^{\rm 3D}}{R_c(l)} = \frac{\Delta}{l^{1/\nu_{\rm 3D}}}. \qquad (10)$$

Note that this relation, being independent of any free parameter, is not a FSS hypothesis but a prediction for the crossover behavior of $R_c(l)$ that satisfies $R_c(1) = R_c^{\rm 2D}$ and $R_c(l \to \infty) = R_c^{\rm 3D}$.

By plugging (10) into (9), one can immediately check that our hypothesis is compatible with the expected 2D FSS behavior for fixed l and large L:

$$\frac{R_c^{\rm eff}(l,L) - R_c(l)}{R_c^{\rm eff}(l,L)} = \frac{A(l)}{L^{1/\nu_{\rm 2D}}}, \qquad (11)$$

with $A(l)$ being the amplitude of the FSS expansion for a system with fixed thickness l:

$$A(l) = \frac{(A-\Delta)l^{1/\nu_{\rm 2D}}}{l^{1/\nu_{\rm 3D}}-\Delta}. \qquad (12)$$

The fit of $R_c^{\rm eff}(l,L)$ data gives $A = 0.63 \pm 0.18$ for the unique fitting parameter in (7). The fitting surface is shown in Fig. 2, and equals all the values of $R_c^{\rm eff}(l,L)$ within their original error bars. Sections of this surface at constant l, showing a good quality of the fit, are presented in Appendix A.

D. Collapsing of size distributions

Having found the values of $R_c(l)$, we return to the collapsing of size distributions predicted by (5), where the product $rl^{1/\nu_{\rm 3D}}$ and the ratio l/L have to be fixed. In Fig. 3(a) we show the collapse obtained for small $l/L = 1/256$, i.e., for lattices that

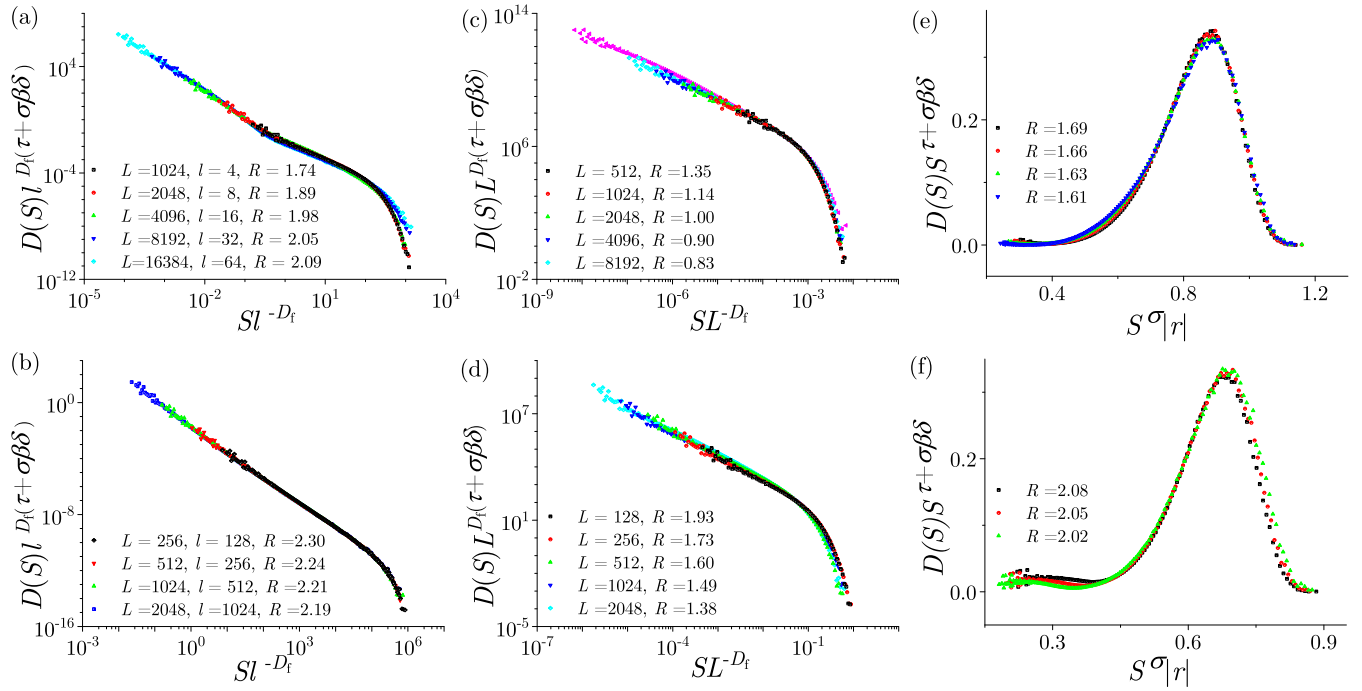

FIG. 3. Data collapsing of the integrated size distributions $D^{(\rm int)}(S)$ predicted by (a, b) (5), (c, d) (13), and (e, f) (14). (a) $l/L = 1/256$. (b) $l/L = 1/2$. (c) $l = 1$, $R_c = 0.54$. (d) $l = 4, R_c = 1.02$. (e) $l = 8$, $L = 4096$. (f) $l = 32$, $L = 4096$. Three-dimensional exponents are used in (a) and (b) because $l = aL$, and 2D exponents are used elsewhere.

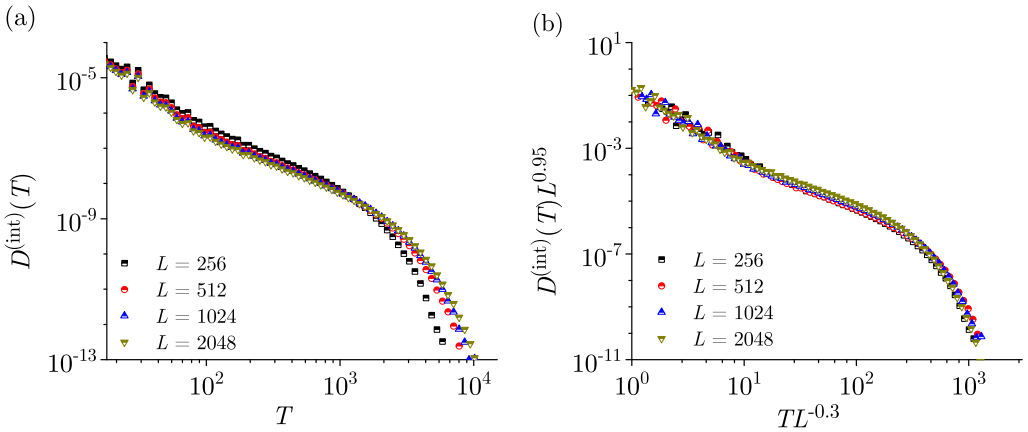

FIG. 4. (a) Duration distributions for several RFIM systems having same the disorder $R = 2.00$ and thickness $l = 16$, but different span L, given in the legend. (b) Overlapping of the distributions, which are shown in (a), is achieved by the spurious values of L exponents (-0.3 along the horizontal axis and 0.95 along the vertical axis). These values just provide deceptive collapsing, and are neither stable (i.e., depend on the range of L) nor related to some true exponents.

are almost planar, while in Fig. 3(b) the collapse is shown for large $l/L = 1/2$ corresponding to almost equilateral 3D lattices; for intermediate cases see Appendix B.

The scaling of size distributions can be also tested along $l =$ const direction (see Fig. 2), in which case the scaling prediction reads

$$D^{(\mathrm{int})}(S;r,1/L,1/L,1/l) = L^{-(\tau+\sigma\beta\delta)D_f} D^{(\mathrm{int})}(S/L^{D_f}; rL^{1/\nu},1,1,L/l). \quad (13)$$

Two examples of such collapsing are shown in Figs. 3(c) and 3(d), where D_f is the fractal dimension of the 2D spanning avalanches in the 2D model [20], and all exponents are also for the 2D model [15,17], because here the system behaves effectively as a 2D system due to constant thickness l. Finally, in Figs. 3(e) and 3(f), we present the most usual collapses (see, for instance, [13,15]) given by

$$D^{(\mathrm{int})}(S;r,1/L,1/L,1/l) = S^{-(\tau+\sigma\beta\delta)} \bar{\mathcal{D}}^{(\mathrm{int})}_{\pm}(S^{\sigma}|r|, S^{\sigma\nu}/L, S^{\sigma\nu}/L, S^{\sigma\nu}/l), \quad (14)$$

and corresponding to $l =$ const and $L =$ const in each set. For similar statements that hold for distributions of other avalanche parameters, like avalanche durations or avalanche energies, see Appendix C.

IV. DISCUSSION

In the studies of the 3D-2D crossover for the Ising model in thermal equilibrium, expressions similar to Eq. (10) were proposed. The exponent accompanying l was initially called the shift exponent, but it was later found to be equal to $1/\nu_{3D}$ [6]. Nevertheless the proposed expressions always had some corrections when l was not large enough. Surprisingly, in our out-of-equilibrium case, we see that (7) is valid in the entire range $l \geqslant 2$.

Our findings, presented so far, may be relevant for the experimental data analysis. In experiments, some relevant parameters can be hardly controllable (or even unaccessible) like, for example, the amount of disorder in the samples that are used in Barkhausen noise (BN) measurements [21–23]. More specifically, a lot of BN experimental analyses are performed on the sets of samples, each containing specimens that are cut at different lengths (5–30 cm) from the same commercial thin ribbon (25–50 μm thick). We expect that such thin samples should give distributions (see Fig. 3 in [24]) that are a mixture of small 3D avalanches, continued by quasi-2D avalanches characterized not by 3D but by 2D critical exponents, like those from our simulations shown in Fig. 4(a). We further expect that the length of tails of these distributions is dominantly influenced by the sample geometry, and less through the (very small) demagnetization factor, inversely proportional to the sample length. Finally, regarding the data collapsing, we mention that according to our predictions the distributions of BN from the samples differing only in length cannot be, strictly speaking, collapsed because that would require their disorders to be different. More problematically, one may even achieve a "reasonable" collapsing of the data pertaining to the same disorder, but at the price of using some spurious exponents, as is illustrated in Fig. 4(b).

Finally, regarding the variation of the size exponents τ that was reported in the theoretical study of the 3D to 2D crossover in Barkhausen noise [25], based on the single-interface model originally proposed in [26], let us note that, at the current numerical precision, we were not been able to detect with certainty analogous variation in the RFIM, due to limited computational facilities. Nevertheless, this could be a subject of our future studies.

V. CONCLUSION

In this paper we have presented the regularities found in 3D to 2D crossover in the case of nonequilibrium zero-temperature the random-field Ising model with metastable dynamics. We have proposed a finite-size scaling hypothesis for the systems with sizes $L \times L \times l$, leading to expressions for the effective critical disorder $R_c^{\mathrm{eff}}(L,l)$ and the scaling of the avalanche distributions that explain the size-driven critical crossover from two dimensions ($l =$ const, $L \to \infty$) to three dimensions ($l \propto L \to \infty$). Our model has a unique fitting parameter for the whole surface $R_c^{\mathrm{eff}}(l,L)$, has no free parameters for the

behavior of $R_c^{\rm eff}(l, L \to \infty)$, and introduces prerequisites for data collapsing which could be particularly important for proper analysis of experimental data for thin 3D systems.

ACKNOWLEDGMENTS

This paper was supported by the Serbian Ministry of Science Project No. 171027; by the Spanish Ministry of Economy and Competitiveness (Spain) Projects No. MAT2016-75823-R, No. MAT2015-69777-REDT, and No. FIS2015-71851-P; and by Agencia de gestió d'Ajuts Universitaris i de Recerca (Catalonia) Project No. 2014SGR-1307. V.N. received funding from La Caixa Foundation and acknowledges financial support from the Spanish Ministry of Economy and Competitiveness, through the "María de Maeztu" Programme for Units of Excellence in R&D (Project No. MDM-2014-0445).

APPENDIX A: DETAILS OF DETERMINATION OF $N(R;l,L)$ AND $R_c^{\rm eff}(l,L)$

In our simulations we found that, like in 2D systems [20], *at most one* 2D spanning avalanche appears in a single run (recall that we consider as the 2D spanning avalanche an avalanche that spans the system at least in one of the two large dimensions L). The average number per single run of such spanning avalanches $N(R;l,L)$ on $L \times L \times l$ systems with disorder R is, for fixed l and L, a function of disorder R, shortly denoted as $N(R)$. In its transition region, this function decays from 1 to 0, see Fig. 5, and can be described by formula (6), where $\mathrm{erfc}(x) \equiv (2/\sqrt{\pi}) \int_x^\infty e^{-t^2} dt$ is the complementary error function centered at inflection point $R = R_0$, and W is the width of the transition disorder region in which $N(R)$ falls from $N \approx 0.76025$ to ≈ 0.23975. As W tends to zero when $L \to \infty$, one may say that the central value R_0 defines the *effective critical disorder* $R_c^{\rm eff}(l,L)$, such that if L is large enough then the 2D spanning avalanches appear, roughly speaking, only at disorders $R \leqslant R_c^{\rm eff}(l,L)$.

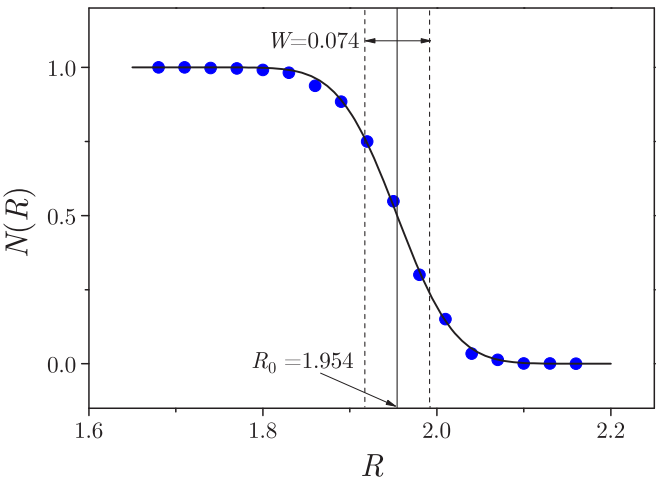

FIG. 5. $N(R)$ vs disorder R, where $N(R)$ is the average number per single run of 2D spanning avalanches triggered in $L \times L \times l$ systems with disorder R. Symbols show $N(R)$ obtained in our simulations for $l = 16$ and $L = 256$. The full curve shows the model function $N_{R_0,W}(R)$ of type (6) that best fits simulation data when $R_0 = 1.954 \pm 0.001$ and $W = 0.074 \pm 0.002$. The position of R_0 is indicated by the full vertical line, and the width W of the transition region is indicated by dashed lines.

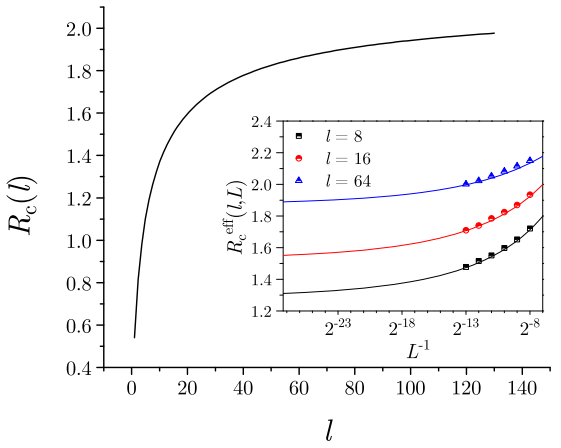

FIG. 6. Critical disorder $R_c(l)$ for the the $L \times L \times l$ family of lattices in the $L \to \infty$ limit, shown vs lattice thickness l. Inset: Symbols show the values of effective critical disorder $R_c^{\rm eff}(l,L)$ vs L^{-1} for l fixed to 8, 16, and 64; error bars are smaller than symbol size. For the same fixed values of l, solid lines show the curves $R_c^{\rm th}(l,L)$, converging to $R_c(l)$ when $1/L \to 0$.

For fixed l, the effective critical disorder $R_c^{\rm eff}(l,L)$ decreases when L increases, and when L becomes infinitely large tends to some limit which can be rightly identified as the critical disorder $R_c(l)$ for the the $L \times L \times l$ family of lattices.

The values of $R_c(l)$, defined as

$$R_c(l) = \lim_{L\to\infty} R_c^{\rm eff}(l,L)\,,$$

are to be determined from the $R_c^{\rm eff}(l,L)$ data with the aid of some extrapolating function. We found that for fixed l our prediction $R_c^{\rm th}(l,L)$, see Eq. (7), is suitable for this purpose, as is illustrated in the inset of Fig. 6. The values of $R_c(l)$, obtained from $R_c^{\rm th}(l,L)$ in the $L \to \infty$ limit, are shown in the main panel of Fig. 6, and are given by Eq. (10) containing no free parameters.

APPENDIX B: COLLAPSING OF INTEGRATED SIZE DISTRIBUTIONS IN THE WHOLE l/L = const RANGE

The collapsing of integrated distribution $D^{(\rm int)}(S;r,1/L,1/L,1/l)$ of avalanche size S follows from the scaling (5), which we repeat for the reader's convenience:

$$D^{(\rm int)}(S;r,1/L,1/L,1/l) = l^{-(\tau+\sigma\beta\delta)D_f} D^{(\rm int)}(S/l^{D_f}; rl^{1/\nu}, l/L, l/L, 1). \quad \text{(B1)}$$

Here, all critical exponents and the fractal dimension of nonspanning avalanches $D_f = 2.78$ are for the 3D model on equilateral lattices, and the values of $rl^{1/\nu}$ and l/L have to be maintained constant for all collapsing distributions. This collapsing was shown in Fig. 3 only for two extreme cases in our simulations: $l/L = 1/256$ (almost planar lattices) in part (a), and $l/L = 1/2$ (almost equisized lattices) in part (b).

Now, in Fig. 7 we show the same type of collapsing for almost all intermediate values of l/L, indicating that prediction

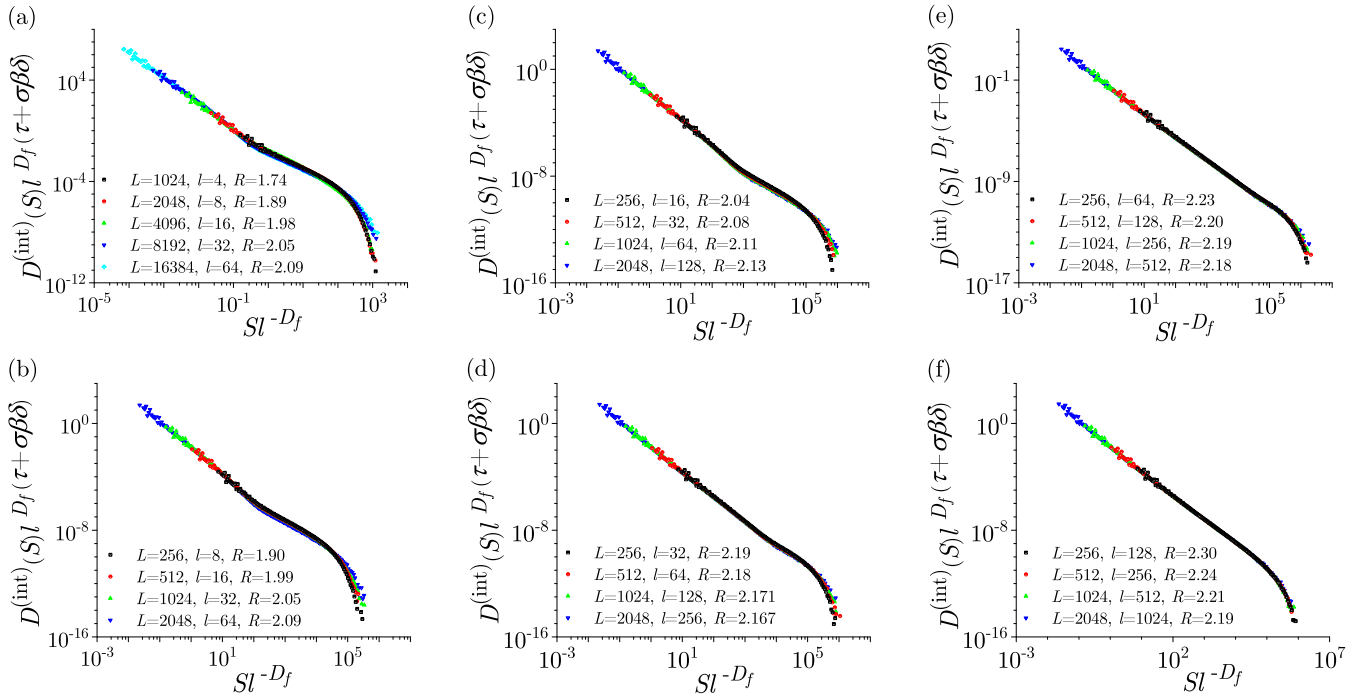

FIG. 7. Data collapsing of the integrated size distributions $D^{(\mathrm{int})}(S)$ predicted by (5). The data are obtained in simulations of systems containing up to $\approx 1.7\times10^{10}$ spins. Parts (a) and (f) are already shown in the main text as parts (a) and (b) of Fig. 5, and are repeated here for the sake of completeness. (a) $l/L = 1/256$. (b) $l/L = 1/32$. (c) $l/L = 1/16$. (d) $l/L = 1/8$. (e) $l/L = 1/4$. (f) $l/L = 1/2$.

(5) holds throughout the entire 3D to 2D crossover region. Regarding this range, we remark that the ratio of l/L smaller than $1/256$ would exceed our computational (and time) limits (e.g., for $l/L = 1/512$ we would need $L = 32\,768$, so the system would contain $\approx 7\times10^{10}$ spins).

APPENDIX C: SCALING OF THE DISTRIBUTIONS OF AVALANCHE DURATIONS AND AVALANCHE ENERGIES

Like for the size distributions, the 3D to 2D crossover is also manifested in distributions of other avalanche parameters.

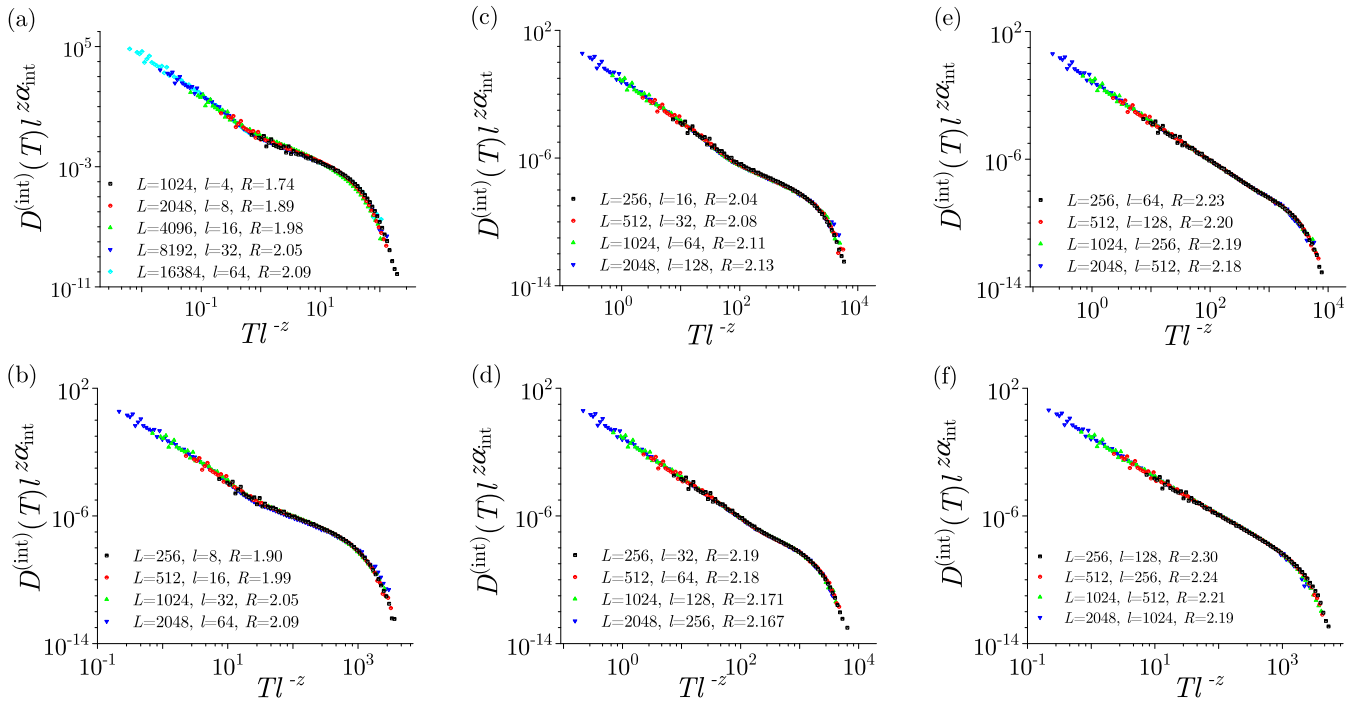

FIG. 8. Data collapsing of the integrated duration distributions $D^{(\mathrm{int})}(T)$ predicted by (C2). The range of l/L, and the values of disorder, are the same as in Fig. 7.

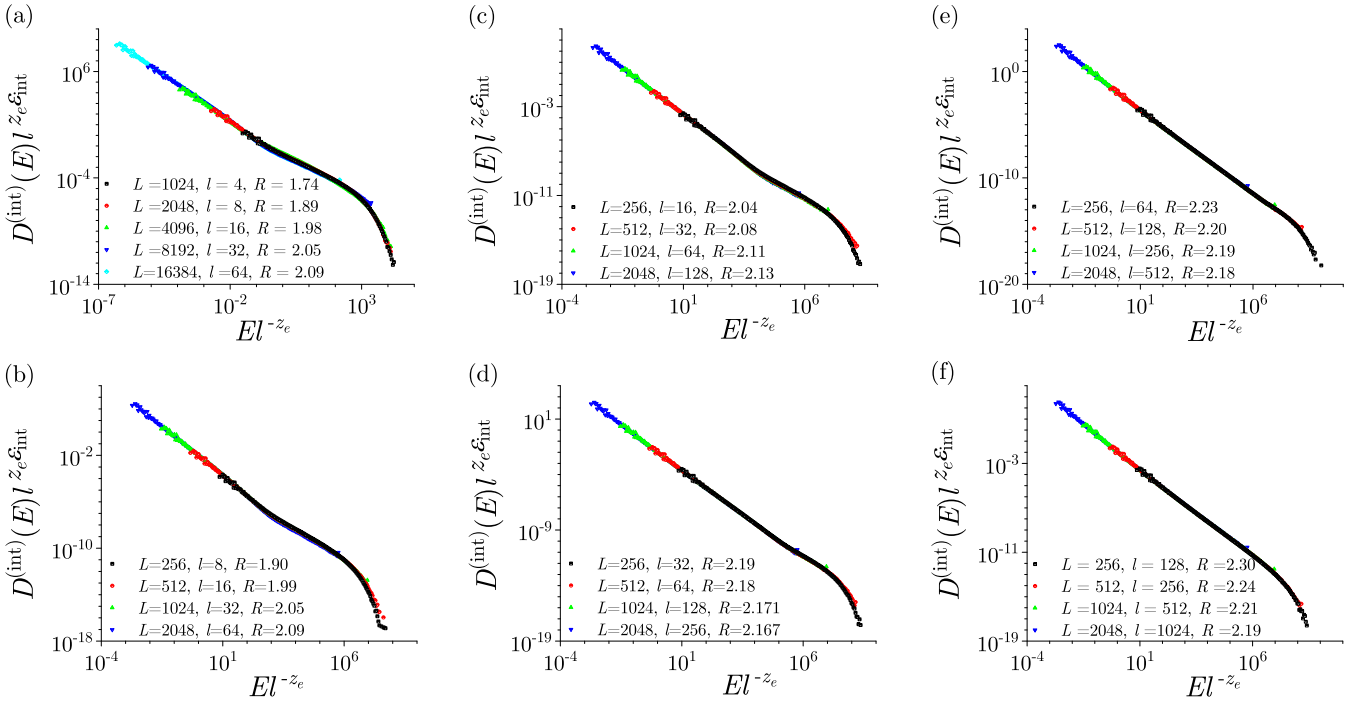

FIG. 9. Data collapsing of the integrated energy distributions $D^{(\mathrm{int})}(E)$ predicted by (C5). The range of l/L, and the values of disorder, are the same as in Figs. 7 and 8.

Avalanche duration T (i.e., time taken for the avalanche to occur) and avalanche energy E (sum of S_t^2, where S_t is the number of spins flipped at time t, with $1 \leqslant t \leqslant T$) are important avalanche parameters that are often measured in RFIM studies. Thus, in the case of avalanche duration, its maximum value $T_{\max}$ for small avalanches should be

$$T_{\max} \propto l^{z} \,, \tag{C1}$$

where z is the dynamical critical exponent in the 3D model. The scaling of avalanche duration distributions reads

$$D^{(\mathrm{int})}(T; r, 1/L, 1/L, 1/l) = l^{-z\alpha_{\mathrm{int}}} D^{(\mathrm{int})}(T/l^{z}; rl^{1/\nu}, l/L, l/L, 1), \tag{C2}$$

where $\alpha_{\mathrm{int}} = \alpha + \sigma\beta\delta(\alpha - 1)/(\tau - 1)$ is the critical exponent for integrated duration distribution, and α is the critical exponent for avalanche duration distribution, $D(T) \propto T^{-\alpha}$. In (C1) and (C2), the exponents z, α_{int}, and ν are the 3D exponents, and their values (together with the values of the 3D exponents α, σ, β, δ, and τ used to calculate α_{int}) are from [14]. The scaling collapse, predicted by (C2), is shown in Fig. 8 in the same range of l/L, and the same values of disorder as in Fig. 7.

Similarly, one should expect that the maximum value $E_{\max}$ of energy of small avalanches should scale as

$$E_{\max} \propto l^{z_e} \,, \tag{C3}$$

where

$$z_e \equiv \frac{\tau - 1}{\sigma\nu(\varepsilon - 1)} \tag{C4}$$

is the dynamical critical exponent for avalanche energy, and that the energy distribution should scale as

$$D^{(\mathrm{int})}(E; r, 1/L, 1/L, 1/l) = l^{-z_e\varepsilon_{\mathrm{int}}} D^{(\mathrm{int})}(E/l^{z_e}; rl^{1/\nu}, l/L, l/L, 1). \tag{C5}$$

Here, $\varepsilon_{\mathrm{int}}$ is the critical exponent for integrated energy distribution, $D^{(\mathrm{int})}(E) \propto E^{-\varepsilon_{\mathrm{int}}}$, which expressed via other exponents reads $\varepsilon_{\mathrm{int}} = \varepsilon + \sigma\beta\delta(\varepsilon - 1)/(\tau - 1)$, where ε is the critical exponent for avalanche energy distribution, $D(E) \propto E^{-\varepsilon}$, the value of which stems from the scaling relation $\epsilon = 1 + (\tau - 1)/(1 - \sigma\nu z)$, see (18) in [17], and the values for 3D exponents τ, σ, ν, and z from [14]. The scaling collapse, predicted by (C5), is shown in Fig. 9 in the same range of l/L, and the same values of disorder as in Figs. 7 and 8.

[1] D. Spasojević, S. Bukvić, S. Milošević, and H. E. Stanley, Phys. Rev. E **54**, 2531 (1996).

[2] F. Huang, M. T. Kief, G. J. Mankey, and R. F. Willis, Phys. Rev. B **49**, 3962 (1994).

[3] G. Z. dos Santos Lima, G. Corso, M. A. Correa, R. L. Sommer, P. C. Ivanov, and F. Bohn, Phys. Rev. E **96**, 022159 (2017).

[4] L. L. Liu and H. E. Stanley, Phys. Rev. Lett. **29**, 927 (1972).

[5] K. Binder, Thin Solid Films **20**, 367 (1974).

[6] K. Kaneda, Y. Okabe, and M. Kikuchi, J. Phys. A **32**, 7263 (1999).

[7] K. W. Lee, J. Korean Phys. Soc. **40**, L398 (2002); K. W. Lee and C. E. Lee, Phys. Rev. B **69**, 094428 (2004).

[8] Y. Laosiritaworn, J. Poulter, and J. B. Staunton, Phys. Rev. B **70**, 104413 (2004).

[9] V. Navas-Portella and E. Vives, Phys. Rev. E **93**, 022129 (2016).
[10] B. Tadić, Physica A **493**, 330 (2018).
[11] I. Balog, G. Tarjus, and M. Tissier, arXiv:1710.04032v1 (2017).
[12] J. P. Sethna, K. A. Dahmen, and O. Perković, in *The Science of Hysteresis*, edited by G. Bertotti and I. Mayergoyz (Academic Press, Amsterdam, 2006); E. K. H. Salje and K. A. Dahmen, Annu. Rev. Condens. Matter Phys. **5**, 233 (2014); D. P. Belanger and T. Nattermann, in *Spin Glasses and Random Fields*, edited by A. P. Young (World Scientific, Singapore, 1998).
[13] J. P. Sethna, K. Dahmen, S. Kartha, J. A. Krumhansl, B. W. Roberts, and J. D. Shore, Phys. Rev. Lett. **70**, 3347 (1993); K. A. Dahmen and J. P. Sethna, *ibid.* **71**, 3222 (1993); Phys. Rev. B **53**, 14872 (1996).
[14] O. Perković, K. A. Dahmen, and J. P. Sethna, Phys. Rev. Lett. **75**, 4528 (1995); arXiv:cond-mat/9609072v1 (1996); Phys. Rev. B **59**, 6106 (1999).
[15] D. Spasojević, S. Janićević, and M. Knežević, Phys. Rev. Lett. **106**, 175701 (2011).
[16] D. Spasojević, S. Janićević, and M. Knežević, Europhys. Lett. **76**, 912 (2006).
[17] D. Spasojević, S. Janićević, and M. Knežević, Phys. Rev. E **84**, 051119 (2011).
[18] F. J. Pérez-Reche and E. Vives, Phys. Rev. B **67**, 134421 (2003); **70**, 214422 (2004).
[19] In order to achieve sufficient numerical precision in our simulations, the number of runs per single disorder ranged from 16 for the largest systems (containing more than 17×10^9 spins), up to 60 000 for the smallest systems. To this end, we had to use speed and memory optimized algorithms and nonstandard numerical techniques.
[20] D. Spasojević, S. Janićević, and M. Knežević, Phys. Rev. E **89**, 012118 (2014).
[21] J. S. Urbach, R. C. Madison, and J. T. Markert, Phys. Rev. Lett. **75**, 4694 (1995).
[22] G. Durin and S. Zapperi, in *The Science of Hysteresis*, edited by G. Bertotti and I. Mayergoyz (Academic Press, Amsterdam, 2006).
[23] J. Xu, D. M. Silevitch, K. A. Dahmen, and T. F. Rosenbaum, Phys. Rev. B **92**, 024424 (2015).
[24] S. Zapperi, P. Cizeau, G. Durin, and H. E. Stanley, Phys. Rev. B **58**, 6353 (1998).
[25] S. L. A. de Queiroz, Phys. Rev. E **69**, 026126 (2004).
[26] J. S. Urbach, R. C. Madison, and J. T. Markert, Phys. Rev. Lett. **75**, 276 (1995).